Archives of Acoustics Vol. 50, No. 2, pp. 235–242 (2025), https://doi.org/10.24425/aoa.2025.153658

Research Paper

# Determination of the Elastic Constant of the Top Plate of a Cello in the Interaction with the Bridge

Pablo PAUPY[(1)*], Pablo TABLA[(2)], Dario HUGGENBERGER[(1)], Federico ELFI[(1)], Eneas N. MOREL[(2),(3)], Jorge R. TORGA[(2),(3)]

[(1)] *Grupo de Vibraciones, Facultad Regional Delta, Universidad Tecnológica Nacional* Campana, Buenos Aires, Argentina

[(2)] *Grupo de Fotónica Aplicada, Facultad Regional Delta, Universidad Tecnológica Nacional* Campana, Buenos Aires, Argentina

[(3)] *Consejo Nacional de Investigaciones Científicas y Técnicas* CABA, Buenos Aires, Argentina

[*]Corresponding Author e-mail: ppaupy@frd.utn.edu.ar

*Received July 13, 2024; revised January 29, 2025; accepted February 6, 2025; published online April 7, 2025.*

This paper aims to determine the equivalent static elastic constant of a cello's top plate in the interaction with the bridge. Experimental results detailing this constant are presented based on measuring the deformation and forces caused by a system of calibrated springs in similar conditions to that obtained when these forces are produced by the action of the strings. Subsequent tests are conducted following an intervention by a luthier to adjust the sound post, with the aim of assessing the impact on the elastic constants.

**Keywords:** elasticity; organology; cello bridge; musical acoustics; boundary conditions; interferometry.



## 1. Introduction

The main function of the cello bridge is to transform the vibrations generated in the strings into vibrations of the top plate. The strings transmit this vibration to the bridge at the points of contact between the two elements, and the bridge transmits it to the top plate through the two supporting feet. The way the bridge performs this transmission and what its modes of vibration are like, are central issues in the final characteristics of the instrument and have been studied by several authors. Minnaert and Vlam (1937) published a pioneering work, where the normal, flexural, and torsional modes of the bridge were studied. Later, in 1963, Steinkopf introduced basic mechanical models of the bridge to obtain the frequency response (Cremer, 1984). Bissinger (2006) carried out studies of various violin bridges and a detailed analysis of the bridge as a filter in the transmission of vibrations to the top plate of the instrument. Among the works with experimental results, Reinicke and Cremer (1970) can be mentioned as one of the first to use optical interferometric techniques to measure vibrations in the instrument. Subsequently, Jansson *et al.* (1994) made interesting contributions to the experimental analysis of violin body vibrations and their effects on the frequency response. In (Jansson, 2004) the importance of the shape and dimensions of the bridge base and foot on the characteristics of the coupling with the top plate of the instrument is determined, demonstrating a correlation between the quality of the violin and the shape of the bridge. Other researchers have analysed the frequency response of the bridge by studying the admittance or mobility variables of the system (Boutillon, Weinreich, 1999; Elie *et al.*, 2013; Malvermi *et al.*, 2021). Simplified shapes of the instrument or some of its parts were modelled and the frequency response was measured or simulated, taking the bridge as a simple mass-spring system or considering more complex models (Woodhouse, 2005; 2014).

In a separate line of research, the impact of the violin and cello bridge shapes on their static and vibrational characteristics was examined through parametric modelling and simulations utilizing the finite element methods. An important point in these works is the boundary conditions to which the bridge is subjected in contact with the top plate of the instrument during normal operation. These conditions ranged from a fixed point to more realistic systems incorporating combinations of springs and dampers. Several models were considered where each foot of the bridge had up to three translational springs and three rotational springs (Kabała *et al.*, 2018). Lodetti's *et al.* (2023) work served as a basis for a subsequent analysis on a cello.

The primary objective of this paper was to measure the static elastic constant of the instrument's top plate at the contact points with each of the bridge's support feet. The proposal aimed to measure the value of the elastic constant in the primary direction of displacement, which is perpendicular to the instrument's top plate, understanding this parameter is crucial as it plays a significant role in determining the boundary conditions that the bridge experiences at the contact points with the top plate.

Another goal of this study was to compare the values of the elastic constants measured at the aforementioned contact points, in two different scenarios: in the first, when the instrument is received from the factory; and in the second, after an adjustment made by a professional luthier. Industrially manufactured cellos are often assembled in music stores, and such assembly frequently requires additional adjustments by professional luthiers. These adjustments significantly influence the elastic conditions between the bridge and top plate. This step is crucial to ensure that the structural and acoustic characteristics of the instrument meet higher standards. As the measurements show, the values of the elastic constant after the luthier's work are considerably lower than before the adjustment, particularly at the treble foot (next to the sound post).

The experimental work was conducted on a setup that include the entire instrument under controlled laboratory conditions, with measurements of the elastic constant taken to assess the variation at different points along the top plate. This variation is due to the structural asymmetry present in both the bridge and the instrument's top plate. The asymmetry was influenced by the curvature of the upper part of the bridge and the stiffness disparity resulting from the positioning of the sound post near the treble support ('A' string 220 Hz), and the bass-bar close to the bass support ('C' string 65.4 Hz).

## 2. Experimental setup

To obtain the values of the elastic constants, an experimental setup was implemented to measure the deformation of the top plate as a function of the force applied at a series of selected points on the instrument top plate. The deformation of a spring of known elastic constant was used to measure the force and a low coherence optical interferometer was used to measure the deformation distances. With this experimental scheme, deformation measurements were carried out under different conditions and results were obtained for the elastic constants at the selected points. From these measurements it was possible to verify a linear behaviour between the displacement and the force in the range of values of both magnitudes to which the instrument is subjected during its execution.

The strings used for this experiment, replacing the original ones, are Jargar® Classic Medium strings. The manufacturer gives the nominal tension of each string (C: 13.8 kg, G: 13.4 kg, D: 14.0 kg, A: 17.9 kg) under normal tuning conditions, with the tension values of the treble strings being higher than those of the bass strings.

The points where the top plate deformation was measured are close to the bridge support points. To ensure clarity, they are identified with numbers 1 to 6. Point 1 is located next to the footrest corresponding to the treble string (note A3 220 Hz) on the tailpiece side of the instrument. Point 2 is located on the right side of the bridge, always seen from the tailpiece side; point 3 on the side of the fingerboard opposite to the location of point 1 and so on in correlative order for points 4, 5, and 6 on the foot corresponding to the bass string. Figure 1 shows the location of these points on the top plate of the instrument.

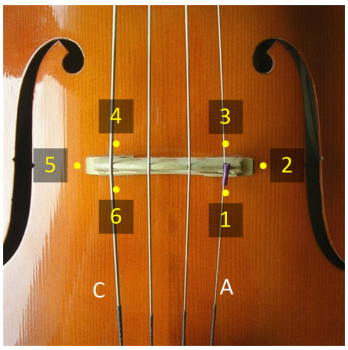


Fig. 1. Strain measurement points indicated on the top plate of the instrument.

Both, the experimental device for measuring force and deformation and the instrument used as sample, were mounted on an anti-vibration table that allows to isolate the system from mechanical noise and external vibrations. A structure was designed and constructed to secure the instrument to the table, providing support for the components used to apply and measure the compression force on the instrument's soundboard, as well as for the corresponding deformation measurement system.

### 2.1. Instrument fixing system

Clamping the instrument on the test table was carried out with a device specifically designed with three purposes. The first was to ensure that the instrument is statically fixed to the table so that the deformations measured are due exclusively to the deformation of the top plate and not to movements of the instrument with respect to the measuring point. The second was to use this structure for the location of the devices intended to exert and measure the force on the top plate and the corresponding deformation measuring device. The third was to preserve the instrument and develop a method of attachment and mounting that would not damage its structure.

The points where the straps are attached to the instrument's C's were used as a link to the fixation structure as they were considered to be structurally stronger. A mechanical clamp element was designed and constructed with separate upper and lower jaws. The lower part is screwed to the measuring table and the upper part presses the instrument top plate as shown in Fig. 2. Both the lower and upper-part press on wooden blocks covered with plush that are in direct contact with the instrument. In this way, the instrument is supported by this clamp system and no other parts are in direct contact with the measuring table. The points set out in the four blocks are the only elements linking the instrument to the measuring table. Figure 2 shows the instrument placed on the measuring table and the top plate compression system in the measuring situation.

Fig. 2. Cello mounted on the measuring table by means of the clamping frame.

### 2.2. Device for exerting and measuring forces

To exert and measure the compression force on the top plate of the instrument, two identical mechanical devices were designed and built to replace the original bridge and were placed at the same support points. In this configuration the cello is stripped of the bridge, tailpiece, and strings. Each of these devices has a support point on the top plate of the instrument, a cylinder with a piston associated to a calibrated thread of 1 mm of advance per turn, and an internal spring of known elastic constant ($k_R$) as it is showed in Fig. 3.

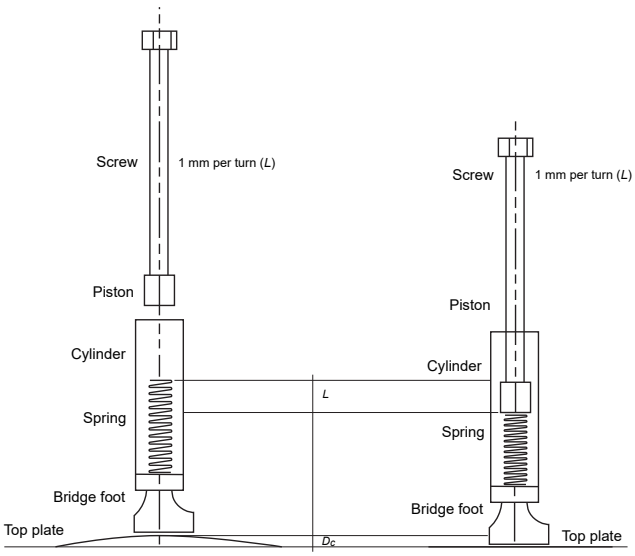


Fig. 3. Device diagrams to exert and measure the compression force on the top plate of the instrument.

To exert a controlled force, the piston is rotated a certain number of revolutions ($n$) compressing the spring at a distance $L$. At the other end of the spring, the support point exerts the same force on the instrument top plate. As a result, it deforms and moves a distance $D_C$, assuming the same behaviour that it has in the tuning and playing process. It is convenient to define the rate of deformation of the top plate per revolution ($A_{pr}$) of the cylinder as

$$A_{pr} = \frac{D_C}{n}. \tag{1}$$

Considering that the calibrated thread pitch is one millimetre per revolution ($10^{-3}$ m/rev) with an error that we estimate at 1 %; the distance $L$ can be expressed as

$$L \pm \Delta L = 10^{-3}\frac{\mathrm{m}}{\mathrm{rev}} * n \pm \left(10^{-5}\frac{\mathrm{m}}{\mathrm{rev}} * n + 10^{-3}\frac{\mathrm{m}}{\mathrm{rev}}\Delta n\right), \tag{2}$$

where $\Delta n$, the error in the number of turns, was obtained from the relation that defines $A_{pr}$:

$$\Delta n = \frac{\Delta D_C}{A_{pr}} + \frac{D_C}{A_{pr}^2}\Delta A_{pr}. \tag{3}$$

The force exerted by the spring ($F_R$) at both ends can be expressed as

$$F_R \pm \Delta F_R = (k_R \pm \Delta k_R) \cdot ((L \pm \Delta L) - (D_C \pm \Delta D_C)), \tag{4}$$

where $k_R$, the elastic constant of the spring, was obtained by measuring the stretch produced by a series of standard weights in the range of values comparable to the stretch measured in tuning.

The average of these measurements, taken as the final value with a relative error of 1.6 %, was

$$k_R = (6100 \pm 100)\,\frac{\mathrm{N}}{\mathrm{m}}.$$

### 2.3. Deformation measurement with an interferometer

Deformation measurements of the top plate surface were made using frequency domain optical coherent tomography (FD-OCT) with a Fizeau-type fiber optic configuration (Vakhtin *et al.*, 2003), as shown in Fig. 4a. This configuration allows measurements at points close to the feet of the bridge and allows simultaneous measurement of the deformation at two points. The interference between the optical reflection generated at the end of each optical fibre (*Fa* and *Fb*) and the reflections on the cello top plate allow to determine the distances between the end of the fiber and the top plate (*Da* and *Db*) as shown in Fig. 4b. *Da* represents the distance measurements taken at points 1 and 6, while *Db* represents the same measurements for points 4 and 3. The distances at points 2 and 5 were calculated as the average of the distances measured at 1 and 3, and 4 and 6, respectively.

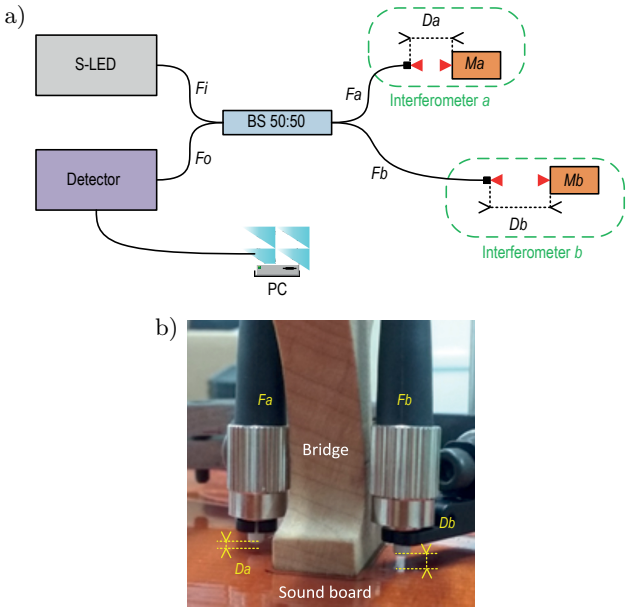


Fig. 4. a) Interferometer schematic. The light emitted by the S-LED source is coupled to the beam splitter (BS 50:50) whose outputs, fibers *Fa* and *Fb*, illuminates the cello top plate. *Da* and *Db* are the distance between each fiber and the top plate. Beams reflected are coupled back into the fibers and sent to the detector through the fiber *Fo*; b) image of the optically instrumented cello.

## 3. Results

The process of measuring and determining the elastic constants of the top plate was carried out in three stages.

In the first stage, only the nominal displacements of the top plate produced by the bridge pressure under normal tuning conditions were measured. Deformation measurements were obtained at points 1, 3, 4, and 6 with the instrument mounted with tailpiece and strings. The deformation values at points 2 and 5 were obtained as the average of the values measured at 1 and 3, and 4 and 6, respectively. Measurements under tuning conditions were made by allowing the instrument to rest and noting that after about eight minutes the stabilisation of the deformation was essentially definitive within the instrumental resolution. A measurement immediately after compression and a second measurement after eight minutes of rest were taken as the norm.

In a second stage, the bridge and strings were replaced by a calibrated spring system. The forces applied with this system corresponded to deformation values equal to those obtained in the first stage. In this way, the values of force and deformation were obtained simultaneously in similar conditions to those achieved in the normal use of the instrument.

In a third stage the same measurements and results are presented as in the second stage but after the luthier has adjusted the instrument. The objective is to compare the values of the elastic constant before and after adjustment.

### 3.1. First stage – Measurement of deformation imposed by the tuning of strings (before luthier's work)

Table 1 presents the measurements of top plate deformation ($D_C$) produced during the tuning process in points 1, 3, 4, and 6.

The values labelled 'free' represent the measurements of distances (*Da* or *Db*) taken before tuning. In this state, the strings were completely slack, positioned between the pegs and the tailpiece, and resting on the bridge without any tension. This condition was maintained for more than eight minutes to ensure the top plate was free of residual tension. Measurements were then taken at points 1, 3, 4, and 6 near the bridge supports, establishing a baseline reference position. This static state served as the zero point for quantifying deformation caused by string tension after tuning.

The values in the column 'tuning 1' corresponds to the first measurement of the same distances (*Da* or *Db*) taken immediately after tuning the four strings. Eight minutes later a second measurement of the same distances was taken, referenced as 'tuning 2', and adjusted the four strings again with the micro tuning screw to obtain 'tuning 3', which was considered as the final measurement of distances resulting from tuning. This procedure was performed three times (measures 1, 2, and 3), at each of the points of the top plate.

Table 1. Absolute displacements and deformation at points 1, 3, 4, and 6 during tuning process.

| Type | Free [μm] | Tuning 1 [μm] | Tuning 2 [μm] | Tuning 3 [μm] | $D_{C\text{-}T1}$ [μm] | $D_{C\text{-}T2}$ [μm] | $D_{C\text{-}T3}$ [μm] |
|---|---|---|---|---|---|---|---|
| a) absolute displacements and deformation at point 1 during tuning process | | | | | | | |
| Measure 1 | 789 | 1252 | 1245 | **1256** | 463 | 456 | **467** |
| Measure 2 | 797 | 1255 | 1252 | **1260** | 458 | 455 | **463** |
| Measure 3 | 798 | 1248 | 1245 | **1272** | 450 | 447 | **474** |
| Average | 794.7 | 1251.7 | 1247.3 | **1262.7** | 457.0 | 452.6 | **468.0** |
| Error | 2.8 | 2.0 | 2.3 | **4.9** | 3.9 | 2.9 | **3.3** |
| b) absolute displacements and deformation at point 3 during tuning process | | | | | | | |
| Measure 1 | 712 | 1394 | 1389 | **1402** | 682 | 677 | **690** |
| Measure 2 | 717 | 1396 | 1394 | **1409** | 679 | 677 | **692** |
| Measure 3 | 716 | 1414 | 1411 | **1419** | 696 | 695 | **703** |
| Average | 715.0 | 1401.3 | 1398.0 | **1410.0** | 685.7 | 683.0 | **695.0** |
| Error | 1.6 | 6.6 | 6.9 | **5.1** | 5.4 | 6.2 | **4.2** |
| c) absolute displacements and deformation at point 4 during tuning process | | | | | | | |
| Measure 1 | 1132 | 1790 1787 | **1803** | 658 | 655 | **671** | |
| Measure 2 | 1134 | 1796 | 1791 | **1807** | 662 | 657 | **673** |
| Measure 3 | 1137 | 1807 | 1805 | **1816** | 670 | 668 | **679** |
| Average | 1134.3 | 1797.7 | 1794.3 | **1808.7** | 663.3 | 660.0 | **674.3** |
| Error | 2.6 | 5.1 | 5.6 | **4.0** | 3.6 | 4.1 | **2.5** |
| d) absolute displacements and deformation at point 6 during tuning process | | | | | | | |
| Measure 1 | 1240 | 1888 | 1877 | **1891** | 648 | 637 | **651** |
| Measure 2 | 1249 | 1897 | 1889 | **1906** | 648 | 640 | **657** |
| Measure 3 | 1249 | 1886 | 1880 | **1907** | 637 | 631 | **658** |
| Average | 1246.0 | 1890.3 | 1882.0 | **1901.3** | 644.3 | 636.0 | **655.3** |
| Error | 3.1 | 3.5 | 3.7 | **5.3** | 3.8 | 2.7 | **2.3** |

The values of deformation referenced as '$D_{C\text{-}T1}$', $D_{C\text{-}T2}$', and '$D_{C\text{-}T3}$' were obtained as the difference between 'tunings 1, 2, 3' and 'free' measurements, respectively. The average was taken as the representative value. The final error was obtained from the standard statistical error of the three deformations as indicated in the last column of the table, in the same way as all the errors indicated in the last row. The final tuning deformation result, utilized in subsequent calculations, is underlined.

### *3.2. Second stage – Measurement of deformation imposed by the spring compression system (before luthier's work)*

At this stage, the bridge and strings were replaced by a system of calibrated springs to apply and measure forces on the instrument. The deformation values ($D_C$) obtained in the previous stage were used as a reference to determine the necessary force that must be applied with the spring system in order to generate similar deformations. To apply the required force in each point, it is necessary to determine the value of the relative rate of deformation per revolution ($A_{pr}$) and the number of revolutions ($n$) of the cylinder of the spring device. To obtain these values each spring was compressed three times simultaneously at the points 1, 3, 4, and 6 and left to rest for eight minutes after each adjustment to make the measurements comparable to those made under tuning conditions. Table 2 summarises the three measurements at each point indicating the compression in microns and the number of revolutions between brackets. The average rate per revolution values is reported in the same table.

Table 2. Deformation measurements ($D_C$), number of revolutions ($n$), and the rate of advance per revolution ($A_{pr}$) in each series of measurements.

| | Point 1 | Point 3 | Point 4 | Point 6 |
|---|---|---|---|---|
| Measure 1 – $D_C$ ($n$) | 483 μm (14 rev) | 720 μm (19.5 rev) | 721 μm (9.5 rev) | 674 μm (9.5 rev) |
| Measure 2 – $D_C$ ($n$) | 482 μm (14 rev) | 694 μm (20 rev) | 683 μm (9 rev) | 675 μm (9.5 rev) |
| Measure 3 – $D_C$ ($n$) | 478 μm (14 rev) | 724 μm (20.5 rev) | 675 μm (9 rev) | 656 μm (9 rev) |
| Measure 1 – $A_{pr}$ | 34.50 μm/rev | 36.92 μm/rev | 75.89 μm/rev | 70.95 μm/rev |
| Measure 2 – $A_{pr}$ | 34.43 μm/rev | 34.70 μm/rev | 72.56 μm/rev | 75.00 μm/rev |
| Measure 3 – $A_{pr}$ | 34.14 μm/rev | 35.32 μm/rev | 75.00 μm/rev | 72.89 μm/rev |
| Average – $A_{pr}$ | (34.36 ±0.11) μm/rev | (34.65 ±0.66) μm/rev | (74.48 ±0.99) μm/rev | (74.95 ±1.65) μm/rev |

The equivalent elastic constant of the top plate ($k_T$) can be defined as

$$F_T = k_T D_C. \tag{5}$$

It is assumed that the elastic force exerted by the top plate '$F_T$' is the same as that exerted by the calibrated spring '$F_R$', then:

$$F_R = F_T = k_T D_C = k_R(L - D_C). \tag{6}$$

So, it is possible to obtain the equivalent elastic constant of the top plate and its error as

$$k_T \pm \Delta k_T = \frac{F_R}{D_C} \pm \left(\frac{\Delta F_R}{D_C} + \frac{F_R}{D_C^2}\Delta D_C\right). \tag{7}$$

Finally, we have the results summarised in Table 3.

We estimate the value of the equivalent elastic constant of the top plate under the support of the foot as the average between the values measured at points 1 and 3 for the *La* (A) and for the *Do* (C) string:

$$k_{T(A)} = (171 \pm 12)\,\text{kN/m},$$

$$k_{T(C)} = (75 \pm 5)\,\text{kN/m},$$

with relative errors in the order of 8 % and 7 %, respectively.

### *3.3. Third stage – Measurement of deformation imposed by the spring compression system (after luthier's work)*

In this section, we present the same measurement and calculus procedure as in the second stage but after the work done by a professional luthier adjusting the position and length of the sound post.

The appreciation of the luthier as soon as he worked on the instrument was that the sound post was 'too rigid' and that he had to shorten its length and position. After luthier's work we measured the static elastic constants again noticing that the values obtained were considerably smaller than before, especially in the treble foot (next to the sound post).

Table 4 shows the final deformation measurements of the strings during the tuning process after an intervention of a luthier consisting in the adjustment of the sound post location.

Table 5 repeats the results presented in Table 2 after luthier's intervention.

Table 6 presents a summary of the results obtained after the luthier's intervention. The last row shows a new magnitude, the stiffness reduction ($Sr$), defined as the percentage relative difference in $k_T$ before (second stage) and after (third stage) luthier's intervention. It is clear that the most remarkable reductions occur at points 1 (18 %) and 3 (36 %), where the sound post has the greatest influence.

Table 3. Synthesis of results at points 1, 3, 4, and 6 for top plate deformation ($D_C$), relative advance per turn ($A_{pr}$), estimated number of revolutions to equalize deformations ($n$), displacement length of the calibration spring ($L$), force exerted by the spring ($F_R$), equivalent elastic constant of the top plate ($k_T$), and its relative error (ER).

| | Point 1 | Point 3 | Point 4 | Point 6 |
|---|---|---|---|---|
| $D_C$ [µm] | 468.0 ±3.3 | 695.0 ±4.2 | 674.3 ±2.5 | 655.3 ±2.3 |
| $A_{pr}$ [µm/rev] | 34.36 ±0.11 | 34.65 ±0.66 | 74.48 ±0.99 | 74.95 ±1.65 |
| $n$ [rev] | 13.62 ±0.14 | 20.06 ±0.51 | 9.05 ±0.16 | 8.74 ±0.23 |
| $L$ [mm] | 13.62 ±0.27 | 20.06 ±0.71 | 9.05 ±0.25 | 8.74 ±0.32 |
| $F_R$ [N] | 80.2 ±3.0 | 118.1 ±6.2 | 51.1 ±2.4 | 49.3 ±2.7 |
| $k_T$ [kN/m] | 171.4 ±7.6 | 169.9 ±9.9 | 75.8 ±3.9 | 75.2 ±4.4 |
| ER [%] | 4.4 | 5.8 | 5.2 | 5.9 |

Table 4. Mean deformation with standard and percentage error after luthier's intervention.

| | Point 1 | Point 3 | Point 4 | Point 6 |
|---|---|---|---|---|
| Average – $D_C$ | 513.0 ±4.3 µm | 729.7 ±6.5 µm | 910.7 ±5.0 µm | 859.7 ±12.7 µm |

Table 5. Deformation measurements ($D_C$), number of revolutions ($n$), and the rate of advance per revolution ($A_{pr}$) in each series of measurements after the luthier's intervention.

| | Point 1 | Point 3 | Point 4 | Point 6 |
|---|---|---|---|---|
| Measure 1 – $D_C$ ($n$) | 574 µm (13 rev) | 736 µm (14 rev) | 931 µm (11 rev) | 888 µm (11 rev) |
| Measure 2 – $D_C$ ($n$) | 530 µm (13 rev) | 760.9 µm (14 rev) | 969 µm (11.5 rev) | 855 µm (11 rev) |
| Measure 3 – $D_C$ ($n$) | 522 µm (13 rev) | 750 µm (14.5 rev) | 926 µm (11 rev) | 848 µm (11 rev) |
| Measure 1 – $A_{pr}$ | 44.16 µm/rev | 52.57 µm/rev | 84.64 µm/rev | 80.73 µm/rev |
| Measure 2 – $A_{pr}$ | 40.77 µm/rev | 54.35 µm/rev | 84.26 µm/rev | 77.73 µm/rev |
| Measure 3 – $A_{pr}$ | 40.15 µm/rev | 51.72 µm/rev | 84.18 µm/rev | 77.09 µm/rev |
| Average – $A_{pr}$ | (41.69 ±1.27) µm/rev | (52.88 ±0.79) µm/rev | (84.36 ±0.15) µm/rev | (78.52 ±1.14) µm/rev |

Table 6. Synthesis of results at points 1, 3, 4, and 6 for top plate deformation ($D_C$), relative advance per turn ($A_{pr}$), estimated number of revolutions to equalize deformations ($n$), displacement length of the calibration spring ($L$), force exerted by the spring ($F_R$), equivalent elastic constant of the top plate ($k_T$), relative error (ER), and stiffness reduction ($Sr$) after the intervention of the luthier.

| | Point 1 | Point 3 | Point 4 | Point 6 |
|---|---|---|---|---|
| $D_C$ [µm] | 513.0 ±4.3 | 729.7 ±6.5 | 610.7 ±5.0 | 859.7 ±12.7 |
| $A_{pr}$ [µm/rev] | 41.69 ±1.27 | 52.88 ±0.79 | 84.36 ±0.15 | 78.52 ±1.14 |
| $n$ [rev] | 12.31 ±0.48 | 13.80 ±0.33 | 7.24 ±0.08 | 10.95 ±0.16 |
| $L$ [mm] | 12.31 ±0.60 | 13.80 ±0.47 | 7.24 ±0.15 | 10.95 ±0.27 |
| $F_R$ [$n$] | 72.0 ±4.9 | 79.7 ±4.3 | 40.4 ±1.7 | 61.6 ±2.8 |
| $k_T$ [kN/m] | 140.4 ±10.8 | 109.2 ±7.3 | 66.2 ±3.4 | 71.7 ±4.32 |
| ER [%] | 7.7 | 6.7 | 5.1 | 6.0 |
| $Sr$ [%] | 18 | 36 | 13 | 5 |

We estimate the value of the equivalent elastic constant of the top plate under the foot support corresponding to the string *La* (A) and *Do* (C):

$$k_{T(A)} = (125 \pm 15)\,\text{kN/m},$$
$$k_{T(C)} = (69 \pm 6)\,\text{kN/m},$$

with relative errors in the order of 12 % and 9 %, respectively.

## 4. Conclusions

An experimental system was developed to measure the force and displacement of the cello's top plate at points near the bridge supports and estimate its static elastic constant. Key findings and contributions are summarized as follows:

– measurement methodology:
  a) top plate deformation was measured using low-coherence interferometry, a non-contact optical technique with sub-micron resolution;
  b) the force was applied and measured using a calibrated spring system mounted on a custom-designed device, ensuring minimal spurious deformations and compatibility with standard instrument fixtures;

– phase 2 results:
  a) before the luthier intervention, the measured static elastic constant ($k_T$) varied significantly across the different points [kN/m]:
    * point 1: $k_T$ = 171.4 ±7.6,
    * point 3: $k_T$ = 169.9 ±9.9,
    * point 4: $k_T$ = 75.8 ±3.9,
    * point 6: $k_T$ = 75.2 ±4.4;
  b) error (ER) values ranged from 4.4 % to 5.9 %;

– phase 3 results:
  a) after professional adjustment of the sound post by luthier (who identified excessive rigidity and corrected its position and length), significant reductions in $k_T$ were observed, particularly at point 3 [kN/m]:
    * point 1: $k_T$ = 140.4 ±10.8 (↓ 18 %),
    * point 3: $k_T$ = 109.2 ±7.3 (↓ 36 %),
    * point 4: $k_T$ = 66.2 ±3.4 (↓ 13 %),
    * point 6: $k_T$ = 71.7 ±4.3 (↓ 5 %);
  b) ER values increased slightly (6.0 % to 7.7 %);

– impact of the luthier's intervention:
  a) the most pronounced stiffness reductions occurred near the treble foot up to 36 % in point 3 (string A, adjacent to the sound post), emphasizing the importance of proper sound post positioning and adjustment for achieving optimal elastic properties.

These findings provide valuable insights for cello setup optimization and serve as a reference for modelling the bridge using the finite difference methods. Future work will focus on refining measurement techniques, extending the analysis to additional instruments, and correlating elastic properties with acoustic performance.

This work highlights the significant contribution that the intuition and expertise of luthiers can make to scientific research aimed at understanding the functioning of musical instruments. Collaborative work, combined with the use of new techniques and scientific methods, offers the potential to provide objective insights into subjective aspects, thereby fostering the generation of new knowledge.

The results obtained using low-coherence interferometry suggest that this technique is highly suitable for measuring deformation at different points of the top plate. This paves the way for future studies focusing on other elements of the instrument.

### Acknowledgments

We would like to thank luthier Fabián Santillán for his kindness and willingness to collaborate on the adjustments of the cello.

## References


1. Bissinger G. (2006), The violin bridge as filter, *The Journal of the Acoustical Society of America*, **120**(1): 482–491, https://doi.org/10.1121/1.2207576.
2. Boutillon X., Weinreich G. (1999), Three-dimensional mechanical admittance: Theory and new measurement method applied to the violin bridge, *The Journal of the Acoustical Society of America*, **105**(6): 3524–3533, https://doi.org/10.1121/1.424677.
3. Cremer L. (1984), *The Physics of the Violin*, The MIT Press, England.
4. Elie B., Gautier F., David B. (2013), Analysis of bridge mobility of violins, [in:] *Proceedings of the Stockholm Music Acoustics Conference 2013*, pp. 54–59, https://hal.science/hal-01060528 (access: 3.06.2024).
5. Jansson E., Molin N., Saldner H. (1994), On eigenmodes of the violin – Electronic holography and admittance measurements, *The Journal of the Acoustical Society of America*, **95**(2): 1100–1105, https://doi.org/10.1121/1.408470.
6. Jansson E.V. (2004), Violin frequency response – Bridge mobility and bridge feet distance, *Applied Acoustics*, **65**(12): 1197–1205, https://doi.org/10.1016/j.apacoust.2004.04.007.
7. Kabała A., Niewczyk B., Gapiński B. (2018), Violin bridge vibration – FEM, *Vibrations in Physical Systems*, **29**: 2018021, https://vibsys.put.poznan.pl/_journal/2018-29/articles/vibsys_2018021.pdf (access: 3.06.2024).
8. Lodetti L., Gonzalez S., Antonacci F., Sarti A. (2023), Stiffening cello bridges with design, *Applied Sciences*, **13**(2): 928, https://doi.org/10.3390/app13020928.
9. Malvermi R. *et al.* (2021), Feature-based representation for violin bridge admittances, arXiv, https://doi.org/10.48550/arXiv.2103.14895.
10. Minnaert M., Vlam C.C. (1937), The vibrations of the violin bridge, *Physica*, **4**(5): 361–372, https://doi.org/10.1016/S0031-8914(37)80138-X.
11. Reinicke W., Cremer L. (1970), Application of holographic interferometry to vibrations of the bodies of string instruments, *The Journal of the Acoustical Society of America*, **47**(4B): 131–132, https://doi.org/10.1121/1.1912237.
12. Vakhtin A.B., Kane D.J., Wood W.R., Peterson K.A. (2003), Common-path interferometer for frequency-domain optical coherence tomography, *Applied Optics*, **42**(34): 6953–6958, https://doi.org/10.1364/AO.42.006953.
13. Woodhouse J. (2005), On the "bridge hill" of the violin, *Acta Acustica united with Acustica*, **91**(1): 155–165.
14. Woodhouse J. (2014), The acoustics of the violin: A review, *Reports on Progress in Physics*, **77**(11): 115901, https://doi.org/10.1088/0034-4885/77/11/115901.